Available online at www.sciencedirect.com
ScienceDirect
Journal of Molecular Catalysis A: Chemical 282 (2008) 117–123
JOURNAL OF MOLECULAR CATALYSIS A: CHEMICAL
www.elsevier.com/locate/molcata

Eosin Y-sensitized nitrogen-doped TiO_2 for efficient visible light photocatalytic hydrogen evolution

Yuexiang Li [a,*], Chengfu Xie [a], Shaoqin Peng [a], Gongxuan Lu [b], Shuben Li [b]

[a] *Department of Chemistry, Nanchang University, Nanchang 330031, China*
[b] *State Key Laboratory for Oxo Synthesis and Selective Oxidation, Lanzhou Institute of Chemical Physics, Chinese Academy of Sciences, Lanzhou 730000, China*

Received 20 July 2007; received in revised form 12 October 2007; accepted 5 December 2007
Available online 14 December 2007

Abstract

A nitrogen-doped TiO_2 (N-TiO_2) photocatalyst was prepared by the calcination of the hydrolysis product of $Ti(SO_4)_2$ with aqueous ammonia. Pt was loaded on N-TiO_2 by photodeposition method. A dye-sensitization photocatalyst was prepared by impregnation method with Eosin Y and the platinized N-TiO_2. The prepared samples were characterized by XRD, UV–vis diffuse reflectance spectra (DRS), BET and FT-IR. The visible light activity of the sensitization photocatalysts was evaluated by photocatalytic hydrogen evolution ($\lambda > 420$ nm) in the presence of electron donor triethanolamine (TEOA). The N-TiO_2 has smaller crystalline size and larger specific surface area to enhance the adsorption amount of Eosin Y than TiO_2 prepared by NaOH. Surface oxygen defects produced by nitrogen doping would improve the adsorption of Eosin Y and excited electron to transfer to the conduction band of N-TiO_2. Therefore the visible light activity of the sensitized nitrogen-doped platinized TiO_2 is much higher than that of the sensitized platinized TiO_2. The sensitized nitrogen-doped platinized TiO_2 calcined at 300 °C has the highest visible light activity among the catalysts calcined at various temperatures, whose activity is increased by a factor of 3 compared to that of the sensitized platinized TiO_2 calcined at the same temperature.

Keywords: Photocatalysis; Visible light; Nitrogen-doped TiO_2; Eosin Y; Sensitization; Hydrogen evolution

1. Introduction

Hydrogen is considered to be an ideal energy carrier for future [1]. If we can convert even a tiny fraction of the solar energy reaching the earth into storable chemicals, such as hydrogen, we will solve many of our problems not only in energy, but also the global environmental and political [2]. TiO_2 has been studied extensively for photocatalytic water splitting to produce hydrogen [3]. The difficulty with this semiconductor is its large bandgap energy of 3.2 eV that can only be excited by ultraviolet light with a wavelength of no longer than 387.5 nm, which accounts for only 4% of the incoming solar energy [4]. In order to achieve efficient water splitting by solar light, considerable efforts [5–10] have been invested in developing photocatalysts capable of using the less energetic but more abundant visible light.

The sensitization of TiO_2 has been identified as an effective means for dye-sensitized solar cells [11] and hydrogen evolution. Some dyes have been proved to be efficient sensitizers for hydrogen evolution over Pt/TiO_2, such as Eosin Y [12], merocyanine [13], $Ru(bpy)_3^{2+}$ [14] and coumarin [15]. In these sensitization reactions, it was important that the sensitizing dye molecule is adsorbed on the TiO_2 particles. The influences of loading various noble metal and CuO on visible light induced hydrogen generation over the dye-sensitized M/TiO_2 (M = Pt, Ru, Rh and CuO) photocatalysts were investigated [16,17]. The strong adsorption of Eosin Y on the loading metal and CuO enhances the efficiency of hydrogen generation.

Except for TiO_2, SnO_2 [18], $H_4Nb_6O_{17}$ [15], silica gel [19], nanotube $Na_2Ti_2O_4(OH)_2$ [20] and Ti-MCM-41 [21] were used as dye-sensitized matrixes for hydrogen production. These matrixes were found to be active for hydrogen evolution under visible light irradiation, despite their function being not completely the same.

Asahi et al. [22] found that nitrogen-doped TiO_2 possesses visible light activity. The nitrogen-doped TiO_2 was prepared

* Corresponding author. Tel.: +86 791 3969983.
E-mail address: liyx@ncu.edu.cn (Y. Li).

1381-1169/$ – see front matter © 2007 Elsevier B.V. All rights reserved.
doi:10.1016/j.molcata.2007.12.005

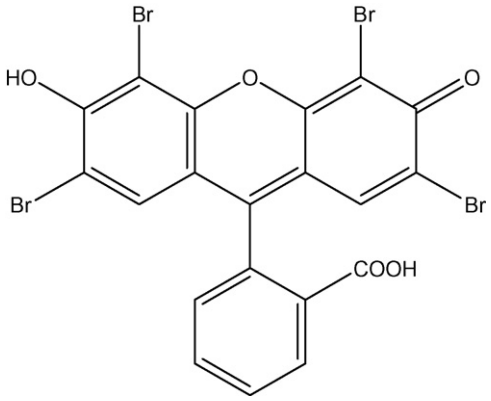

Fig. 1. Molecular structure of Eosin Y.

under the atmosphere of NH_3 gas using commercial TiO_2. Nitrogen-doped TiO_2 was prepared directly in the calcination process of TiO_2 using the method of neutralization hydrolyzation [23]. It has been reported that nitrogen-doped TiO_2 is visible light active for photocatalytic hydrogen evolution [24], but its activity is very low.

In the present study, we used nitrogen-doped TiO_2 as a matrix to prepare a high active dye-sensitization (Eosin Y) photocatalyst. To the best of our knowledge, studies on coupling dye sensitization with nitrogen doping for TiO_2 have not been reported. The activity of Eosin Y-sensitized nitrogen-doped TiO_2 for hydrogen evolution increases notably compared to that of the sensitized TiO_2. The effects of the nitrogen doping for the prepared sensitization catalysts were investigated.

2. Experimental

2.1. Preparation of photocatalyst samples

In this work, an Eosin Y dye supplied by the Sinopharm Group Chemical Reagent Limited Company (China) was used as a photosensitizer of the catalysts. Except that $Ti(SO_4)_2$ was of a chemical reagent grade, the other chemicals were of analytic reagent grade and used without further purification.

Nitrogen-doped TiO_2 was prepared as described in the literature [23]. Twenty-four grams of $Ti(SO_4)_2$ was dissolved in 200 ml distilled water under strong stirring. The pH value of the $Ti(SO_4)_2$ solution was adjusted to 7.2 with aqueous ammonia (25 wt%). After filtrated and washed to remove SO_4^{2-} with distilled water (determined with 0.1 mol l^{-1} $BaCl_2$ solution), the sample was dried at 105 °C and milled in a mortar. Then the samples were calcined at 200 °C, 300 °C, 400 °C, 500 °C, respectively for 2 h to prepare nitrogen-doped TiO_2 (denoted as N-TiO_2). Pure TiO_2 was prepared by the same method for N-TiO_2, except that 1 mol l^{-1} NaOH solution was used as a precipitator instead of aqueous ammonia.

Pt was loaded on photocatalysts by a photodeposition method. 0.753 g TiO_2, 1 ml anhydrous ethanol, 10 ml 1.93×10^{-3} mol l^{-1} H_2PtCl_6 solution and 89 ml distilled water were added into a 190 ml Pyrex cell with a flat window. Other conditions are the same as those in the photocatalytic reaction (see following section). The mixture was irradiated by a 400 W high pressure Hg lamp for 2 h. After filtrated and washed with distilled water, the powders (denoted as Pt-TiO_2, Pt-deposited amount: 0.5 wt%) were dried at 100 °C and milled in a mortar. Pt was deposited on N-TiO_2 (denoted as Pt-N-TiO_2) by the same method.

0.500 g Pt-TiO_2 was added into 20 ml 5.00×10^{-3} mol l^{-1} anhydrous ethanol solution of Eosin Y. The mixture was stirred for 12 h at room temperature in the dark, filtrated and then dried at 100 °C. The obtained sample was denoted as Eosin Y-Pt-TiO_2. The Pt-N-TiO_2 sample was treated by the same method. The obtained sample was denoted as Eosin Y-Pt-N-TiO_2.

2.2. Characterization of photocatalysts

XRD patterns of the prepared photocatalysts were measured on a Britain Bede D1 System multifunction X-ray diffractometer, employing Cu Kα radiation λ = 0.15406 nm. UV–vis DRS were obtained on the spectrophotometer of HITACHI U-3310 equipped with an integrating sphere accessory ($BaSO_4$ was used as a reference). Infrared absorption spectra were measured on a Nicolet 380 FT-IR spectrometer by the transmission method using the KBr pellet technique. The specific surface areas were measured on a ST-08 surface analyzer by the volumetric BET method using nitrogen as adsorbent.

Adsorption amounts of Eosin Y on TiO_2 and N-TiO_2 were measured as follows. 0.300 g catalyst was added into 12 ml 5.00×10^{-3} mol l^{-1} anhydrous ethanol solution of Eosin Y. The mixture was stirred for 12 h at room temperature in the dark. After filtration, the concentration of Eosin Y in the filtrate was measured at 524 nm on a spectrophotometer. The adsorption amount of Eosin Y onto catalyst was calculated based on the concentration difference (ΔC) before and after the mixing.

2.3. Photocatalytic activity under visible light irradiation

Photocatalytic reactions were conducted in a 190 ml Pyrex cell with a flat window for illumination. A 400 W high pressure Hg lamp was used as the light source. The light source was equipped with a cutoff filter (λ > 420 nm) to remove radiation below 420 nm and to ensure illumination of visible light only. Typically, 0.100 g of catalyst was suspended in 80 ml 0.79 mol l^{-1} triethanolamine solution (pH 7.0, adjusted by 1:1 HCl). Prior to irradiation, the suspension of the catalyst was dispersed in an ultrasonic bath for 5 min and N_2 was bubbled through the reaction mixture for 30 min to completely remove oxygen. The photocatalytic activity was determined by measuring the amount of hydrogen produced for 2 h irradiation on a gas chromatography (TCD, 13× molecular sieve column, N_2 as gas carrier).

3. Results and discussion

3.1. Crystallinity and specific surface of both TiO_2 and N-TiO_2 samples

Fig. 2 shows the XRD patterns of various N-TiO_2 samples calcined at different temperatures. N-TiO_2-300 °C, N-TiO_2-400 °C

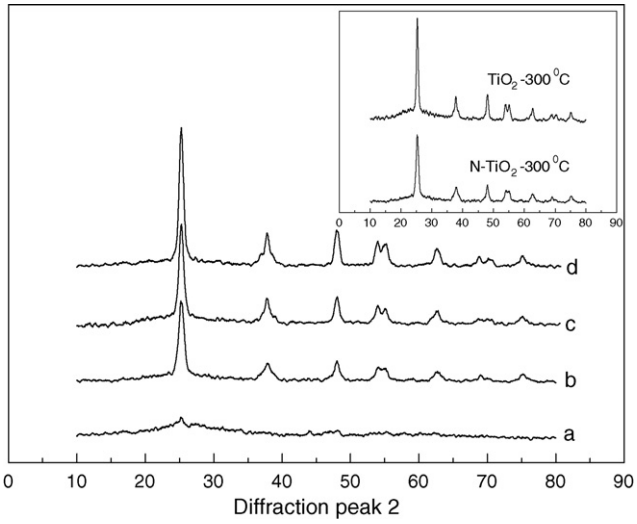

Fig. 2. XRD patterns of N-TiO_2 samples calcined at different temperatures: (a) N-TiO_2-200 °C; (b) N-TiO_2-300 °C; (c) N-TiO_2-400 °C; (d) N-TiO_2-500 °C.

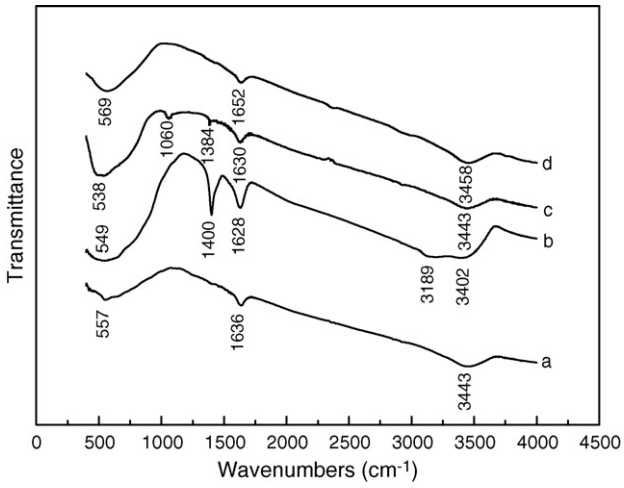

Fig. 3. FT-IR spectra of nitrogen-doped TiO_2 and TiO_2 calcined at 200 °C and 300 °C: (a) TiO_2-200 °C; (b) N-TiO_2-200 °C; (c) N-TiO_2-300 °C; (d) TiO_2-300 °C.

and N-TiO_2-500 °C are only consisted of anatase, whereas N-TiO_2-200 °C exists mainly in amorphism. With calcination temperature increasing, the diffraction peaks of N-TiO_2 become sharper, and thus their crystallinity increases. There is no diffraction peak of Ti–N compound, which can be attributed to that the amount of the doped nitrogen is very small.

The inset of Fig. 2 shows the XRD patterns of TiO_2-300 °C and N-TiO_2-300 °C. No remarkable difference between both samples was observed except diffraction intensity. The diffraction peaks of TiO_2-300 °C are sharper than that of N-TiO_2-300 °C, indicating that the crystallinity of the former is higher than that of the latter.

The crystalline size, D, was calculated by following Scherrer's formula:

$$D = \frac{0.9\lambda}{\beta_{1/2}\cos\theta}$$

where λ is the wavelength (nm) of characteristic X-ray applied, $\beta_{1/2}$ is the half-value width of anatase (1 0 1) peak obtained by XRD and θ is 25.3/2.

The as-calculated particle size of samples b, c, d and TiO_2-300 °C are 14.7 nm, 18.0 nm, 24.6 nm and 21.1 nm, respectively. Thus it can be concluded that the particle size of TiO_2 prepared by using aqueous ammonia as a precipitator is smaller than that by using NaOH solution.

Table 1 shows the specific surface area of TiO_2 and N-TiO_2 powders calcined at different temperatures. With calcination temperature increasing, the specific surface areas of both TiO_2 and N-TiO_2 decrease, but the specific surface area of TiO_2 decreases faster than that of N-TiO_2 and the effect is more notable at higher temperature. This can be attributed to that ammonia species adsorbed on TiO_2 plays an important role to restrain the growth of the crystal particle in process of the calcination. Thus the specific surface area of N-TiO_2 increases compared to that of TiO_2, which is consistent with the result from the XRD analysis. At higher calcined temperature (such as at 500 °C), release of the doped nitrogen by oxidation under air atmosphere [25] would also restrain growth of the crystal particle to increase the specific surface area.

Table 1
Specific surface area of TiO_2 and N-TiO_2 calcined at different temperatures

Sample	Specific surface area ($m^2\ g^{-1}$)			
	200 °C	300 °C	400 °C	500 °C
TiO_2	78.06	70.47	53.85	22.97
N-TiO_2	99.53	92.60	81.32	59.27

3.2. Behavior of nitrogen doping

Fig. 3 shows the infrared absorption spectra of TiO_2 and N-TiO_2 calcined at 200 °C and 300 °C. There are mainly three absorption bands in the region of 520–580 cm^{-1}, 1630–1640 cm^{-1}, 3420–3450 cm^{-1} for the four samples. The absorption bands in the region of 3420–3450 cm^{-1}, 1630–1640 cm^{-1} are assigned to the stretching vibration and bending vibration of the hydroxyl on surface of TiO_2 catalyst, respectively. The absorption band in the region of 520–580 cm^{-1} is assigned to the stretching vibration of Ti–O [26].

Compared with TiO_2-200 °C (sample a), two new absorption peaks of N-TiO_2-200 °C (sample b) at 3189 cm^{-1} and 1400 cm^{-1} appear, which can be assigned to the N–H stretching vibration and the N–H bending vibration of NH_4^+, respectively [25]. The N–H stretching vibration and the N–H bending vibration of NH_3 are 3458 cm^{-1} and 1646 cm^{-1}, respectively [27]. This indicates that ammonia species is absorbed on N-TiO_2-200 °C in form of NH_4^+ instead of NH_3. For N-TiO_2-300 °C (sample c), the absorption peaks of NH_4^+ disappear almost and a new absorption peak at 1060 cm^{-1} appears, which indicates that some nitrogen atoms have replaced the oxygen atoms of TiO_2 crystal lattice to form yellow nitrogen-doped TiO_2, and the absorption peak can be assigned to the N–Ti–O stretching vibration [26]. Thus we are sure that nitrogen doping does not take place at 200 °C, but very effectively at 300 °C.

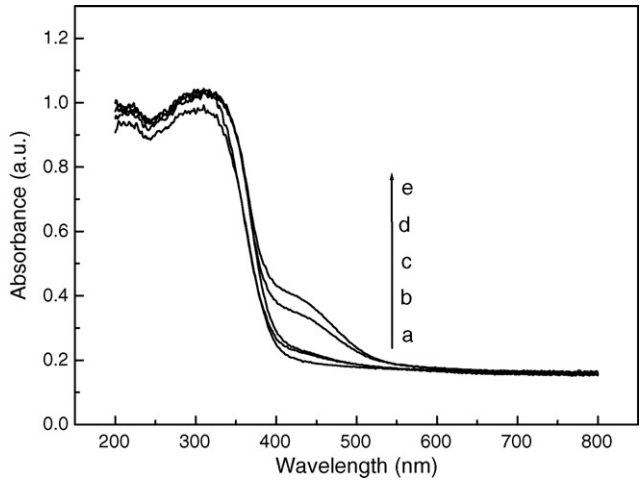

Fig. 4. UV–vis DRS of TiO_2-300 °C and N-TiO_2 samples calcined at different temperature: (a) TiO_2-300 °C; (b) N-TiO_2-200 °C; (c) N-TiO_2-500 °C; (d) N-TiO_2-400 °C; (e) N-TiO_2-300 °C.

Compared N-TiO_2-300 °C (sample c) with TiO_2-300 °C (sample d), the stretching vibration peak at 3458 cm^{-1} shifts to low wavenumber (at 3443 cm^{-1}), whereas the stretching vibration peak at 569 cm^{-1} shifts to low wavenumber (at 538 cm^{-1}). With nitrogen doping, oxygen vacancies are easily created in grain boundaries [23]. The shifts of the two peaks would be attributed to forming the N–Ti–O and oxygen vacancies.

3.3. Photoabsorption property of both TiO_2 and N-TiO_2

Fig. 4 shows the UV–vis diffuse reflectance absorption spectra of samples TiO_2-300 °C, N-TiO_2-200 °C, N-TiO_2-300 °C, N-TiO_2-400 °C and N-TiO_2-500 °C. It can be seen that the absorption of TiO_2-300 °C is limited only to ultraviolet light region, whereas the absorption threshold value of N-TiO_2-300 °C is extended from 380 nm to 570 nm and the absorption edge of it shifts toward low wavenumber 10 nm. The absorption intensity in the region of 400–600 nm of N-TiO_2 samples gradually decreases in the order of N-TiO_2-300 °C > N-TiO_2-400 °C > N-TiO_2-500 °C > N-TiO_2-200 °C (without doped nitrogen).

The colours of the prepared nitrogen-doped TiO_2 calcined at 200 °C, 300 °C, 400 °C, and 500 °C were white, deep yellow, yellow and pale yellow, respectively. With the temperature increasing, release of the doped nitrogen would be accelerated by oxidative reaction under air atmosphere [25]. Thus, the amount of the doped nitrogen is the highest at 300 °C, and decreases from 300 °C to 500 °C. When calcined temperature is 200 °C, nitrogen is not doped into TiO_2 crystal lattice.

3.4. Adsorption of Eosin Y

Table 2 shows the adsorption amount of Eosin Y on TiO_2 and N-TiO_2 powders calcined at different temperatures. The adsorption amounts of Eosin Y on TiO_2 and N-TiO_2 increase with calcination temperature decreasing, except the samples calcined at 200 °C. Sample N-TiO_2-200 °C having comparatively smaller adsorption amount would be attributed to that there was a large amount of NH_4^+ on TiO_2. The adsorption amount of Eosin Y on N-TiO_2 is about two times higher than that of TiO_2 at the same calcination temperature.

Table 2
Adsorption amount of Eosin Y on TiO_2 and N-TiO_2 calcined at different temperatures

Sample	Adsorption amount of Eosin Y (μmol g^{-1})			
	200 °C	300 °C	400 °C	500 °C
TiO_2	86.67	82.22	74.44	56.67
N-TiO_2	160.00	172.22	146.67	124.44

Fig. 5 shows the UV–vis diffuse reflectance absorption spectra of Eosin Y-TiO_2-300 °C and various Eosin Y-N-TiO_2 samples calcined at different temperatures. The sensitization of Eosin Y extends the visible light response range of both TiO_2 and N-TiO_2 compared to Fig. 4. Eosin Y makes TiO_2 and N-TiO_2 have a very strong absorption in region of 400–600 nm. The absorption intensity of Eosin Y-N-TiO_2-300 °C (sample e) is much higher than that of Eosin Y-TiO_2-300 °C (sample a). The absorption intensity in the region of 400–600 nm of Eosin Y-N-TiO_2 samples decreases in the order of Eosin Y-N-TiO_2-300 °C (sample e) > Eosin Y-N-TiO_2-200 °C (sample d) > Eosin Y-N-TiO_2-400 °C (sample c) > Eosin Y-N-TiO_2-500 °C (sample b), which is consistent with the result from Table 2.

Fig. 6 shows the UV–vis diffuse reflectance absorption spectra of various Eosin Y-Pt-N-TiO_2 samples calcined at different temperatures. Compared Fig. 5 with Fig. 6, the absorption spectra of the Eosin Y-Pt-N-TiO_2 samples are similar to these of the Eosin Y-N-TiO_2 samples, but the baselines of the former are raised, which would be attributed to Pt loading. Pt loading amount on Eosin Y-Pt-N-TiO_2 samples is only 0.5 wt% and the adsorption of Eosin Y should be small [16], thus we would assume that Eosin Y was mainly adsorbed at N-TiO_2 (TiO_2).

We measured UV–vis diffuse reflectance absorption spectra of the aged Eosin Y-TiO_2-300 °C and Eosin Y-N-TiO_2-300 °C

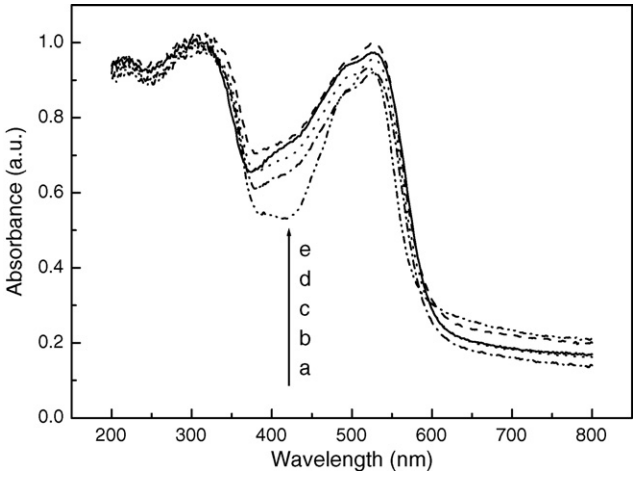

Fig. 5. UV–vis DRS of N-TiO_2 samples calcined at different temperatures with the sensitization of Eosin Y: (a) Eosin Y-TiO_2-300 °C; (b) Eosin Y-N-TiO_2-500 °C; (c) Eosin Y-N-TiO_2-400 °C; (d) Eosin Y-N-TiO_2-200 °C; (e) Eosin Y-N-TiO_2-300 °C.

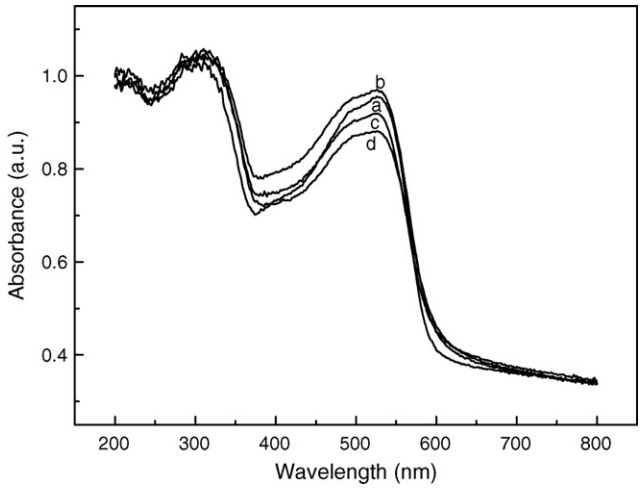

Fig. 6. UV–vis DRS of Pt-N-TiO_2 samples calcined at different temperatures with the sensitization of Eosin Y: (a) Eosin Y-Pt-N-TiO_2-200 °C; (b) Eosin Y-Pt-N-TiO_2-300 °C; (c) Eosin Y-Pt-N-TiO_2-400 °C; (d) Eosin Y-Pt-N-TiO_2-500 °C.

samples after 1 month in the dark. The UV spectra of the aged samples kept unchanged compared to the fresh samples, indicating that Eosin-Y was stable under our experiment condition.

3.5. Comparison of photocatalytic activity

Fig. 7 shows the photocatalytic activities for hydrogen evolution over various Eosin Y-Pt-TiO_2 and Eosin Y-Pt-N-TiO_2 samples. For the Eosin Y-Pt-TiO_2, the activity decreases in the order of 300 °C > 200 °C > 400 °C > 500 °C, whereas for the Eosin Y-Pt-N-TiO_2, 300 °C > 400 °C > 200 °C > 500 °C. The activities of both Eosin Y-Pt-TiO_2-300 °C and Eosin Y-Pt-N-TiO_2-300 °C are the highest among the corresponding samples calcined at various temperatures, and the activity of Eosin Y-Pt-N-TiO_2-300 °C is increased by a factor of 3 compared to that of Eosin Y-Pt-TiO_2-300 °C.

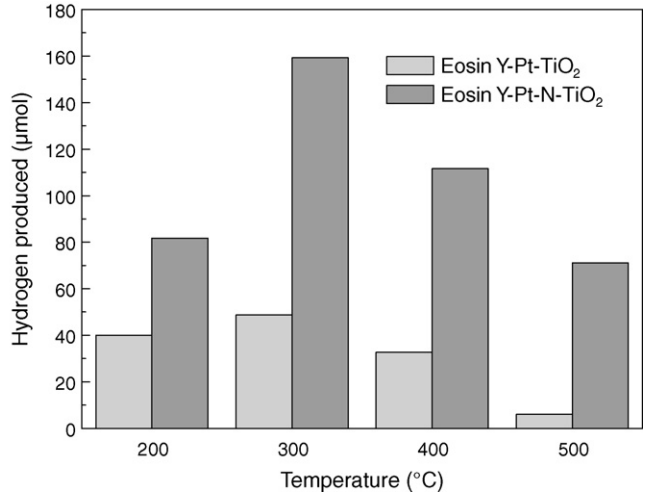

Fig. 7. Effect of prepared temperature of photocatalysts on photocatalytic hydrogen evolution under visible light (λ > 420 nm) irradiation. Reaction conditions: irradiation time, 2 h; 80 ml 0.79 mol l^{-1} TEOA solution, pH 7.0.

Both Eosin Y in the TEOA solution under visible light irradiation and EosinY-Pt-N-TiO_2 in the dark did not produce hydrogen, meaning that Eosin Y-Pt-N-TiO_2 has a good activity. The activity of N-TiO_2 and Pt-N-TiO_2 samples (without sensitization) is too low to be observed, indicating that activity of Eosin Y-Pt-N-TiO_2 originates only from the sensitization. Only small amounts of hydrogen (2–3 μmol for 1 h) were produced over samples Eosin Y-TiO_2-300 °C and Eosin Y-N-TiO_2-300 °C under our experiment condition, suggesting that Pt is very important to hydrogen evolution.

3.6. Discussion for the high activity of Y-Pt-N-TiO_2

Photocatalytic reaction mechanism of hydrogen generation over Eosin Y-sensitized Pt-loaded TiO_2 and N-TiO_2, and effects of nitrogen doping are speculated as follows. Under visible light irradiation, the Eosin Y dye molecule absorbs visible light and electrons of the dye are excited from the HOMO to the LUMO state. The excited electrons transfer to the conduction band of TiO_2 and N-TiO_2, and then to the Pt nanoparticles. Because Pt nanoparticles are the hydrogen active sites, the electrons concentrated on Pt nanoparticles participate in photocatalytic water reduction into hydrogen. Eosin Y can be adsorbed preferentially at Pt [20], other than at the surface of TiO_2. Thus the excited Eosin Y can also transfer electron directly to the Pt particle to produce hydrogen, which would be the second way for hydrogen evolution. The dye molecule would regenerate in the electron donor (TEOA) solution.

According to the structure of Eosin Y molecule (Fig. 1), there are one carboxyl group and phenol hydroxyl group. Eosin Y adsorbed on the TiO_2 or N-TiO_2 may be present in two forms: a hydrogen-bonded physisorbed species and a chemisorbed alkoxide species. The dye having carboxylic group could be fixed by ester-like linkage at TiO_2 (surface Ti) in organic solvent [12], and could also adsorbed at TiO_2 water interface by docking of the carboxylic group [28]. Phenol hydroxyl group can be fixed to surface titanium atom by esterification [29]. Thus we would assume Eosin Y would be mainly adsorbed chemically on the TiO_2 or N-TiO_2 via carboxyl group and phenol hydroxyl group. In general, there is a large amount of hydroxyl groups on TiO_2 surface, for example, P 25 TiO_2 with a specific surface area of 55 $m^2\ g^{-1}$ having a large surface hydroxyl group capacity (0.46 mmol g^{-1}) [30]. Based on data from Table 2, it would be assumed that only a small part of hydroxyl groups on TiO_2 or N-TiO_2 surface would react with the carboxyl group and phenol hydroxyl group of the dye to fix it.

Fig. 8 shows the infrared absorption spectra of TiO_2-300 °C, Eosin Y-TiO_2-300 °C, N-TiO_2-300 °C, Eosin Y-N-TiO_2-300 °C and Eosin Y. Compared the spectrum of the sample a with that of the sample b, it can be observed that the hydroxyl stretching vibration peak of TiO_2 at 3458 cm^{-1} shifts to low wavenumber (at 3444 cm^{-1}) by the sensitization of Eosin Y, which would be attributed to that Eosin Y was chemically fixed at TiO_2 via its carboxyl group and phenol hydroxyl group.

Theory calculation shows that N impurities are found to be more stable in the sub-surface layers [31]. Experimental evidences prove that the nitrogen is located well below the surface

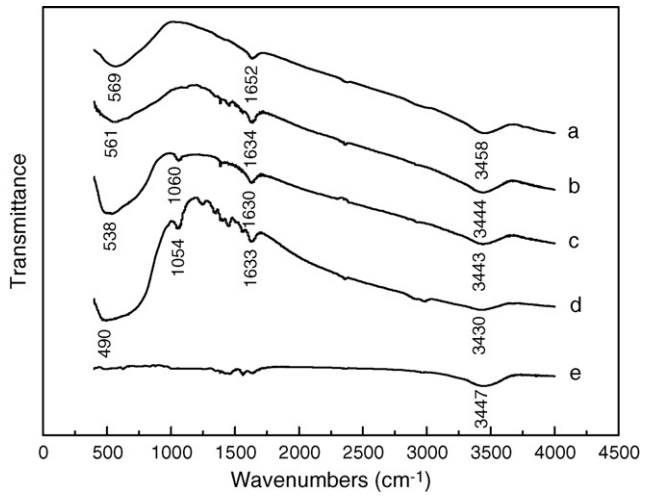

Fig. 8. FT-IR spectra of TiO_2-300 °C and N-TiO_2-300 °C samples with and without the sensitization of Eosin Y: (a) TiO_2-300 °C; (b) Eosin Y-TiO_2-300 °C; (c) N-TiO_2-300 °C; (d) Eosin Y-N-TiO_2-300 °C; (e) Eosin Y.

of N-TiO_2, when N doping is produced by oxidation of the metal nitride [32]. On our experiment condition, samples were calcined under air atmosphere. Thus we can conclude that the doping nitrogen should be located mainly below the surface. The doped nitrogen amount at TiO_2 prepared by the method is very small [23]. Thus the surface nitrogen species and the adsorption of Eosin Y via them on N-TiO_2 should be negligible.

N doping is expected to introduce more oxygen vacancies at the surface than commonly observed for the anatase surface [31]. It was reported that ethylene glycol molecules are preferentially chemisorbed at the defect sites generated during the doping of the N atoms [33]. The carboxyl group and phenol hydroxyl group of Eosin Y should be adsorbed preferentially at the defect sites.

Compared the spectrum of the sample c with that of the sample d, it can be observed that hydroxyl stretching vibration peak, Ti–O–N stretching vibration peak and Ti–O stretching vibration of N-TiO_2 shift to low wavenumber (from 3443 cm^{-1} to 3430 cm^{-1}, from 1060 cm^{-1} to 1054 cm^{-1} and from 538 cm^{-1} to 490 cm^{-1}, respectively) due to the sensitization of Eosin Y, which would be attributed to strong interactions between the carboxyl group and phenol hydroxyl group of Eosin Y, and surface Ti sites and the defect sites of N-TiO_2.

As shown in Fig. 7 and Table 2, the activity of Eosin Y-Pt-N-TiO_2-300 °C is three times higher than that of Eosin Y-Pt-TiO_2-300 °C, whereas the adsorption of N-TiO_2-300 °C is about two times higher than that of TiO_2-300 °C and the specific surface area of the former is only a little larger than that of the latter. The results can be attributed to that the strong interaction between Eosin Y and the surface oxygen defects on N-TiO_2 to largely increase adsorption and reaction properties [33]. It would take place more effectively that the photoinduced electron injection into the conduction band of N-TiO_2 at the surface oxygen defects. Therefore the photocatalytic activity of Eosin Y-Pt-N-TiO_2 is much higher than that of Eosin Y-Pt-TiO_2.

Because there is the largest amount of doped nitrogen for N-TiO_2-300 °C among the N-TiO_2 samples (200–500 °C), we concluded that there would be the largest amount of surface oxygen defects generated by nitrogen doping for N-TiO_2-300 °C. Thus Eosin Y-Pt-N-TiO_2-300 °C having the highest activity would be attributed to its largest amount of surface oxygen defects and higher specific surface area.

4. Conclusion

The dye-sensitization photocatalyst Eosin Y-Pt-N-TiO_2 with high visible activity was prepared. The sensitization of Eosin Y extends the visible light response range of N-TiO_2 and TiO_2. The adsorption amount of Eosin Y at N-TiO_2 increases compared to that at TiO_2 prepared by NaOH. In particular, the surface oxygen defects produced by nitrogen doping would improve adsorption of Eosin Y and the excited electron to transfer to the conduction band of N-TiO_2. Therefore the photocatalytic activity of Eosin Y-Pt-N-TiO_2 is much higher than that of Eosin Y-Pt-TiO_2. On the optimum conditions, the activity of Eosin Y-Pt-N-TiO_2-300 °C is enhanced by a factor 3 compared to that of Eosin Y-Pt-TiO_2-300 °C.

Acknowledgements

The financial support of Department of Sciences and Technology of China (2003CB214503), the National Nature Science Foundation of China (No. 20763006), and the Nature Science Foundation of the Jiangxi Province (No. 0620047) are gratefully acknowledged.

References

[1] M. Anpo, M. Takeuchi, J. Catal. 216 (2003) 505.
[2] K. Kalyanasundaram, M. Graetzel, Coord. Chem. Rev. 248 (2004) 1161.
[3] Y. Li, G. Lu, S. Li, Appl. Catal. A 214 (2001) 179.
[4] A.L. Iinsebigler, G.Q. Lu, J.T. Tates Jr., Chem. Rev. 95 (1995) 735.
[5] Z.G. Zou, J.H. Ye, K. Sayama, H. Arakawa, Nature 414 (2001) 625.
[6] S.U.M. Khan, M. Al-Shahry, W.B. Ingler Jr., Science 297 (2002) 2243.
[7] A. Ishikawa, T. Takata, J.N. Kondo, M. Hara, H. Kobayashi, K. Domen, J. Am. Chem. Soc. 124 (2002) 13547.
[8] I. Tsuji, H. Kato, H. Kobayashi, A. Kudo, J. Am. Chem. Soc. 126 (2004) 13406.
[9] D. Jing, L. Guo, J. Phys. Chem. B 110 (2006) 11139.
[10] Z.B. Lei, W.S. You, M. Liu, G. Zhou, T. Takata, M. Hara, K. Domen, C. Li, Chem. Commun. (2003) 2142.
[11] B.O. Regan, M. Graetzel, Nature 353 (1991) 737.
[12] R. Abe, K. Hara, K. Sayama, K. Domen, H. Arakawa, J. Photochem. Photobiol. A: Chem. 137 (2000) 63.
[13] R. Abe, K. Sayama, Chem. Phys. Lett. 362 (2002) 441.
[14] J. Sabate, S. Cervera-March, R. Simarro, J. Gimenez, Int. J. Hydrogen Energy 15 (1990) 115.
[15] R. Abe, K. Hara, K. Sayama, H. Arakawa, J. Photochem. Photobiol. A: Chem. 166 (2004) 115.
[16] Z. Jin, X. Zhang, G. Lu, S. Li, J. Mol. Catal. A: Chem. 259 (2006) 275.
[17] Z. Jin, X. Zhang, Y. Li, S. Li, G. Lu, Catal. Commun. 8 (2007) 1267.
[18] K. Gurunathan, P. Maruthamuthu, M.V.C. Sastri, Int. J. Hydrogen Energy 22 (1997) 57.
[19] X. Zhang, Z. Jin, Y. Li, S. Li, G. Lu, J. Power Sources 166 (2007) 74.
[20] Q. Li, G. Lu, J. Mol. Catal. A: Chem. 266 (2007) 75.
[21] Q. Li, Z. Jin, Z. Peng, Y. Li, S. Li, G. Lu, J. Phys. Chem. C 111 (2007) 237.
[22] R. Asahi, T. Morikawa, T. Ohwaki, K. Aoki, Y. Taga, Science 293 (2001) 269.
[23] T. Ihara, M. Miyoshi, Y. Iriyama, O. Matsumoto, S. Sugihara, Appl. Catal. B: Environ. 42 (2003) 403.

[24] J. Yuan, M. Chen, J. Shi, W.H. Shangguan, Int. J. Hydrogen Energy 31 (2006) 1326.
[25] T. Matsumoto, N. Iyi, Y. Kaneko, K. Kitamura, S. Ishihara, Y. Takasu, Y. Murakami, Catal. Today 120 (2007) 226.
[26] S. Liu, X. Chen, X. Chen, Chin. J. Catal. 27 (2006) 697.
[27] M.E. Jacox, W.E. Thompson, J. Mol. Spectrosc. 228 (2004) 414.
[28] A. Kornherr, A. Tortschanoff, E. Portuondo-Campa, F. van Mourik, M. Chergui, G. Ziffere, Chem. Phys. Lett. 430 (2006) 375.
[29] S. Ikeda, C. Abe, T. Torimoto, B. Ohtani, J. Photochem. Photobiol. A: Chem. 160 (2003) 61.
[30] M. Herrmann, H.P. Boehm, Z. Anorg. Allg. Chem. 368 (1969) 73.
[31] C.D. Valentin, E. Finazzi, G. Pacchioni, A. Selloni, S. Livraghi, M.C. Paganini, E. Giamello, Chem. Phys. 339 (2007) 44.
[32] A. Orlov, M.S. Tikhov, R.M. Lambert, C. R. Chim. 9 (2006) 794.
[33] T. Tachikawa, Y. Takai, S. Tojo, M. Fujitsuka, H. Irie, K. Hashimoto, T. Majima, J. Phys. Chem. B 110 (2006) 13158.